HOXC10 Suppresses Browning to Maintain White Adipocyte Identity

H.Y. Angeline Tan, M.F. Michelle Sim, Shi-Xiong Tan, Yvonne Ng, Sin Yee Gan, Hongyu Li, Suat Peng Neo, Jayantha Gunaratne, Feng Xu, and Weiping Han

METABOLISM

Promoting beige adipocyte development within white adipose tissue (WAT) is a potential therapeutic approach to staunch the current obesity epidemic. Previously, we identified homeobox-containing transcription factor HOXC10 as a suppressor of browning in subcutaneous WAT. Here, we provide evidence for the physiological role of HOXC10 in regulating WAT thermogenesis. Analysis of an adipose-specific HOXC10 knockout mouse line with no detectable HOXC10 in mature adipocytes revealed spontaneous subcutaneous WAT browning, increased expression of genes involved in browning, increased basal rectal temperature, enhanced cold tolerance, and improved glucose homeostasis. These phenotypes were further exacerbated by exposure to cold or a β-adrenergic stimulant. Mechanistically, cold and β-adrenergic exposure led to reduced HOXC10 protein level without affecting its mRNA level. Cold exposure induced cAMP-dependent protein kinase–dependent proteasome-mediated degradation of HOXC10 in cultured adipocytes, and shotgun proteomics approach identified KCTD2, 5, and 17 as potential E3 ligases regulating HOXC10 proteasomal degradation. Collectively, these data demonstrate that HOXC10 is a gatekeeper of WAT identity, and targeting HOXC10 could be a plausible therapeutic strategy to unlock WAT thermogenic potentials.

Classical brown adipose tissues (BAT) regulate adaptive thermogenesis to transform chemical energy into heat, mediated via mitochondria enriched with uncoupling protein-1 (Ucp-1), resulting in an inducible proton leakage across inner mitochondrial membrane, protecting against hypothermia and obesity (1). Recent recognition using novel radiodiagnosis measures revealed that adult humans possess metabolically functional BAT, and the amount of BAT is inversely correlated with BMI, with the lowest present in obese individuals (2–4). Intriguingly, brownlike adipocytes (known as beige adipocytes), found in clusters within white adipose tissue (WAT) depots, exhibit great plasticity in response to metabolic stimuli, such as cold exposure or β-adrenergic activation, acquiring distinct thermogenic properties to BAT for a full program of thermogenesis and effective energy dissipation (5,6). These beige adipocytes are morphologically similar to brown adipocytes, characterized by multilocular small lipid droplets, *Ucp-1* expression, and Ucp-1–dependent thermogenic capacity (5,7,8). Existing evidence suggests that the presence of brownlike adipocytes at the supraclavicular region of humans exhibits characteristics of beige adipocytes found in mice (9). Indeed, increasing beige adipocytes in WAT enhances energy expenditure and maintains glucose homeostasis in humans (10,11). This increase of intermediate white-to-beige adipocytes in WAT correlates with decreased body fat and resistance to diet-induced obesity (12,13). Therefore, promoting WAT beiging is a potential therapeutic approach to staunch the current obesity epidemic. However, the precise molecular mechanisms underlying beige adipogenesis are not completely understood.

The *Hox* family of homeobox genes (Hox genes) are a class of transcription factors that define the axial patterning of development in vertebrates (14). The Hox genes regulate several fundamental processes through distinct mechanisms, including hematopoiesis, myogenesis, and cardiogenesis (15–18), but its significance in regulating adipocyte biology is not fully elucidated. Among the Hox

S.-X.T. is currently affiliated with the School of Applied Science, Republic Polytechnic, Singapore.

Y.N. is currently affiliated with Atlantis Bioscience Pte Ltd, Singapore.

analogs, *HOXC8* expression is higher in WAT than in BAT and was proposed as a negative regulator of thermogenesis in WAT (19). More recently, a large-scale genome-wide association study identified *HOXC10* association with waist-to-hip ratio (20). Subsequent correlation studies revealed that higher expression of *HOXC9* and *HOXC10* in subcutaneous than in omental adipose tissue samples correlated with body fat mass (21). These observations indicate that beyond their developmental specifications, Hox genes may regulate adipocyte physiology between the two fat types.

We recently identified HOXC10 as a suppressor of browning of subcutaneous WAT (22). *HOXC10* is selectively expressed in subcutaneous white adipocytes in mice. Expression of *HOXC10* in subcutaneous WAT suppressed beiging of WAT and impaired the ability of these mice to maintain body temperature during cold exposure, while deletion of *HOXC10* in adipocytes differentiated from stromal vascular fraction (SVF) of WAT increased thermogenic browning genes, evidenced by elevated Ucp-1 levels in mature adipocytes. HOXC10 exerted its suppressive effect, partially through downregulation of *Prdm16* expression in adipocytes differentiated from WAT SVF. Transcriptional coactivator *Prdm16* is thought to play a key role in WAT browning (6,23). Prdm16 is a short-lived protein and, upon ubiquitination by an unknown E3 ligase, is rapidly degraded by the 26S proteasome pathway (24). Given that HOXC10 interacts with and suppresses Prdm16 expression to control BAT-selective gene expression in WAT and that the deletion of HOXC10 promotes browning of subcutaneous WAT, we considered proteasomal protein quality control as a possible alternative pathway by which proteasomal-mediated *HOXC10* degradation is counterbalanced in adipocytes.

The aim of the current study is to clarify the physiological role of HOXC10 during cold adaptation, leading to enhanced thermogenesis in WAT. We generated an adipose-specific HOXC10 knockout mouse line (AHKO) in which HOXC10 is deleted from mature adipocytes in all adipose depots in adult mice. AHKO mice exhibit spontaneous subcutaneous WAT browning, with enhanced thermogenic *Ucp-1* gene expression at room temperature. Moreover, these mice show higher basal rectal temperature and are more tolerant against prolonged cold exposure, alongside improved glucose homeostasis. Mechanistically, cold exposure leads to increased protein turnover of HOXC10 by promoting proteasome-mediated degradation. Together, these data support HOXC10 as a gatekeeper of white adipocyte identity and suggest HOXC10 as a therapeutic target in unlocking thermogenic potentials of white adipocytes.

RESEARCH DESIGN AND METHODS

Metabolic Studies
Metabolic studies were conducted to assess the effects of targeted deletion of HOXC10. Respiratory exchange ratio (RER), VCO_2, VO_2, physical locomotor activity, and food intake were simultaneously measured for each mouse by using established phenotyping Comprehensive Lab Animal Monitoring System (CLAMS)-Oxymax (Columbus Instruments, Columbus, OH). All measurements were adjusted relative to body weight and lean mass (milliliters per hour per kilogram of lean mass). At the end of dietary interventions, all adipose fat depots were harvested for analysis of thermogenic gene expression via real-time PCR, and terminal bleed via cardiac puncture was performed to measure circulating levels of glucose, insulin, and leptin. Glucose levels in tail blood were measured with an Accu-Chek Advantage Blood Glucose Meter at timed intervals following an intraperitoneal injection of 2 g D-glucose/kg body wt.

Gene Expression Analysis
Total RNA from tissues or cultured cells was isolated and purified using the TRIzol reagent (Invitrogen) and the RNeasy Mini Kit (Qiagen). cDNA was synthesized using RevertAid cDNA Conversion Kit (Fermentas). Relative expression of mRNAs was determined by quantitative PCR using the SYBR Green PCR system (Applied Biosystems), and values were normalized to TATA-binding protein (TBP) levels using the $\Delta\Delta$−threshold cycle method. All primer sequences were previously described in Ng et al. (22).

Body Composition and Histology
Body composition was measured in nonanesthetized mice using MRI (EchoMRI). For histology, fresh adipose tissues were harvested and fixed in 10% neutral-buffered formalin overnight. Paraffin processing, embedding, sectioning, and standard hematoxylin and eosin (H-E) staining were performed.

Statistical Analysis
The data were presented as means ± SEM. Comparisons of data were made by using two-tailed Student t test. Statistical significance was denoted as $*P < 0.05$; $**P \le 0.01$; and $***P \le 0.001$.

Data and Resource Availability
The data sets generated during and/or analyzed during the current study are available from the corresponding author upon reasonable request. The resources generated during and/or analyzed during the current study are available from the corresponding author upon reasonable request.

RESULTS

Adipocyte-Specific Deletion of *HOXC10* Results in Increased Formation of Beige-Like Adipocytes in Subcutaneous WAT of Adult Mice
To investigate the functional role of HOXC10 in mature adipocytes in vivo, we generated a mature AHKO mouse model using adiponectin-Cre mice (Fig. 1A). Accordingly, *HOXC10* mRNA levels were greatly reduced in subcutaneous WAT of AHKO mice when compared with control mice (Fig. 1B). We also verified the successful deletion of HOXC10
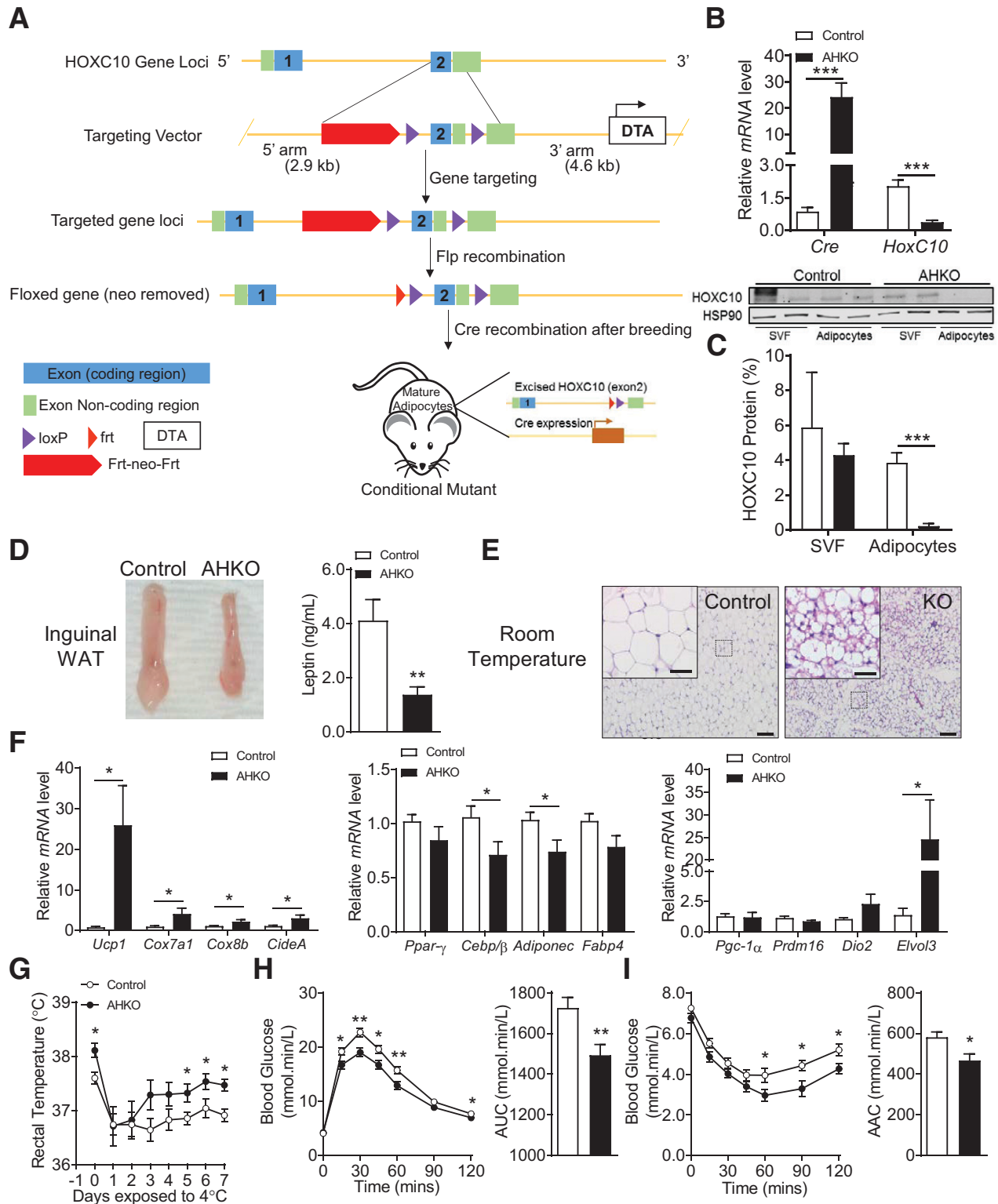
Figure 1—Deletion of AHKO results in widespread accumulation of beigelike adipocytes in subcutaneous WAT depots of AHKO mice. *A*: Targeting strategy for *HOXC10* gene knockout. The targeting vector contained homology arms of 2.9 kb (5' arm) and 4.6 kb (3' arm). The flox sites were located in exon 2. *B*: Relative mRNA levels of *Cre* and *HOXC10* in inguinal WAT (iWAT) of control and AHKO mice (*n* = 10). *C*: Relative protein levels of HOXC10 in SVF and fractionated adipocytes isolated from iWAT of five pooled control and AHKO mice (*n* = 2). HSP90 served as a loading control. *D*: Representative photograph of iWAT and corresponding circulating leptin levels at 20 weeks of age fed on chow diet. *E*: H-E staining of iWAT section. Scale bars = 20 μm. Insets illustrate a magnified view of the figures (scale bars = 100 μm). *n* = 4. *F*: Relative mRNA levels of common adipocyte genes and brown/beige-selective thermogenic markers; *n* = 10. *G*: Body temperature was measured following 7-day cold challenge at 10 weeks of age; *n* = 7. Glucose (*H*) and insulin tolerance test (*I*) of control and AHKO mice between 15 and 16 weeks of age. Data are presented as mean ± SEM. Student *t* test: *$P < 0.05$, **$P < 0.01$, ***$P < 0.001$ (*n* = 10). AAC, area above the curve; AUC, area under the curve; Frt, loxP-flippase recognition target.

protein expression in the mature adipocyte fraction of subcutaneous WAT (Fig. 1C). Consistent with previous observations (25), we observed higher HOXC10 levels in the SVF of subcutaneous WAT.

Homozygous HOXC1-floxed (HOXC10$^{flox/flox}$) control mice appeared normal without obvious phenotypic abnormalities. The growth curves of control and AHKO mice was monitored on chow diet from 4 to 20 weeks of age. Both controls and AHKO exhibited similar body weights and body length as well as body composition at 20 weeks of age (Supplementary Fig. 1A–C). Reduced circulating levels of leptin were observed in AHKO (Fig. 1D), and this reduction commonly corresponds to decreased adiposity (26–28). Intriguingly, AHKO fat mass and the various fat depots examined were not significantly different from wild-type (WT) mice (Supplementary Fig. 1C and D). H-E staining revealed significant widespread multilocular beige adipocytes (Fig. 1E) in the subcutaneous WAT of AHKO mice. Furthermore, adipocyte thermogenic markers, including Ucp-1, Cox7a1, Cox8b, and CideA, were enriched in AHKO subcutaneous WAT (Fig. 1F), indicating that deletion of HOXC10 promotes spontaneous browning of subcutaneous WAT in the absence of metabolic stimulation. The mRNA levels of adipogenic markers Ppar-γ and Fabp4 as well as BAT-enriched transcription factor PGC-1α were not altered, indicating that HOXC10 has minimal effects on adipogenesis. However, Adiponectin and Cebp/β expression levels were decreased in AHKO mice. This reduction of Cebp/β expression in AHKO mice suggests that HOXC10 may be involved in the transcriptional regulation of Cebp/β, which is essential to activate the full thermogenic genetic program in WAT. In addition, the expression levels of Ucp-1–independent thermogenic genes such as Ckmt, Ckb, Serca2b, Fgf21, and Pm20d1 were not altered in AHKO mice (Supplementary Fig. 1E), indicating that HOXC10 exerts its effect primarily through a Ucp-1–dependent pathway in subcutaneous WAT. Prolonged cold exposure induces browning of subcutaneous WAT in rodents (29). Notably, AHKO mice exhibited a higher basal body temperature and were protected against hypothermia during 7 days of cold challenge compared with their control littermates (Fig. 1G), suggesting enhanced adaptive thermogenic capacity in the absence of HOXC10. We also determined glucose regulation by intraperitoneal glucose tolerance test and insulin tolerance test between 15 and 16 weeks of age and found that AHKO mice displayed better glucose tolerance and insulin sensitivity when compared with the control mice (Fig. 1H and I). There was no difference in plasma insulin levels or fed and fasting blood glucose levels between the two groups (Supplementary Fig. 1E and F). Further studies are needed to determine the relative effects of HOXC10 deletion on insulin sensitivity in adipocytes of AHKO mice. We thus hypothesize that AHKO's resistance to cold challenge and improved glucose metabolism could partly be due to altered energy expenditure resulting from the increased formation of beigelike adipocytes in WAT; hence, we used CLAMS to determine the energy consumption of these mice.

HOXC10 Depletion Increases Energy Expenditure as a Result of Enhanced Thermogenesis in Subcutaneous WAT

Our data indicated that HOXC10 deletion results in improved metabolic status despite no differences in body weight or total body fat mass between AHKO and control mice. Furthermore, an increase in brown-fat markers (Fig. 1F) suggested an increase in mitochondrial biogenesis and/or function in AHKO subcutaneous WAT. We subsequently determined the energy consumption using the CLAMS system. Both heat production and VO$_2$ consumption (Fig. 2A and B) were increased in AHKO mice, but there was no difference in RER (Fig. 2C), suggesting that increased energy expenditure in AHKO mice is not due to change in fuel substrate utilization. We also observed a transient increase in nocturnal physical activity, although overall locomotor activity (Fig. 2D) and total body lean mass (Supplementary Fig. 1C) were similar between AHKO and control mice. Although the AHKO mice did not show any significant changes in body weight or fat mass compared with control mice, there is a trend toward decreased body weight gain and decreased fat mass across all adipose tissue depots at later time points (Supplementary Fig. 1A–D). This might explain the apparent energy imbalance due to increased beiging and energy expenditure in the AHKO mice, as described in Figs. 1 and 2. There were no significant differences in food intake between genotypes (Supplementary Fig. 1G), indicating that the enhanced energy expenditure was unlikely the consequence of hyperphagic-induced thermogenesis. The above observations raise the question if deletion of HOXC10 has any impact on BAT function. Given the enormous effect of classical BAT on thermoregulation and metabolic activity, alterations in BAT activity may also impact whole-body energy expenditure in AHKO mice.

To determine the metabolic consequence of HOXC10 deletion on BAT in vivo, HOXC10 was deleted in Myf5-expressing precursor cells by crossing HOXC10$^{flox/flox}$ mice to the Myf5-cre line. Age-matched male controls and conditional deletion (Myf5 HKO) mice were maintained on a standard or high-fat diet (HFD) starting from 6 weeks of age for 15 weeks. On chow diet, no differences were found in body weight or body composition (Supplementary Fig. 2A and B) between the genotypes. Analysis of gene expression demonstrated no significant differences in key thermogenic marker levels in BAT or subcutaneous WAT (Supplementary Fig. 2C and D) on chow diet. Changes in body temperature in response to cold exposure and glucose clearance (Supplementary Fig. 2E–G) were not different between Myf5 HKO and control mice. There was also no difference in energy expenditure, RER, or locomotor activity (Supplementary Fig. 2H–J). Similarly, on HFD, no obvious phenotypic differences
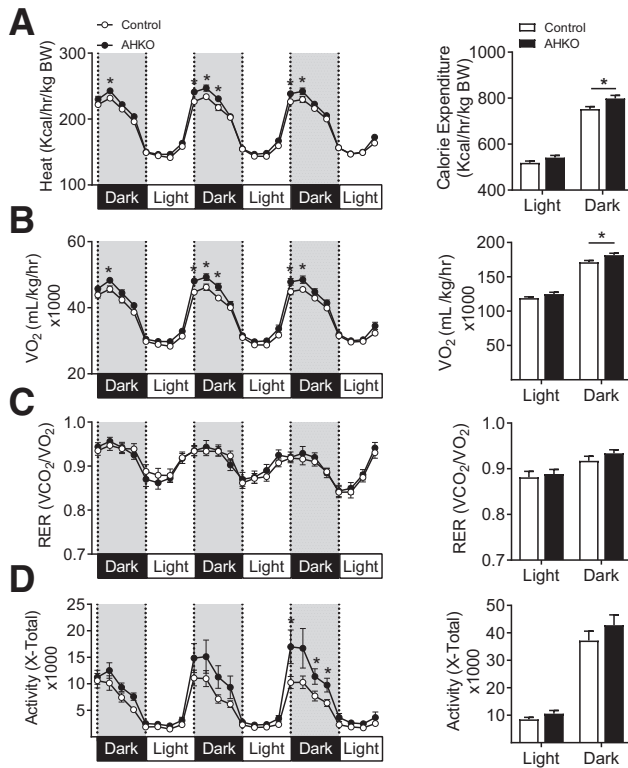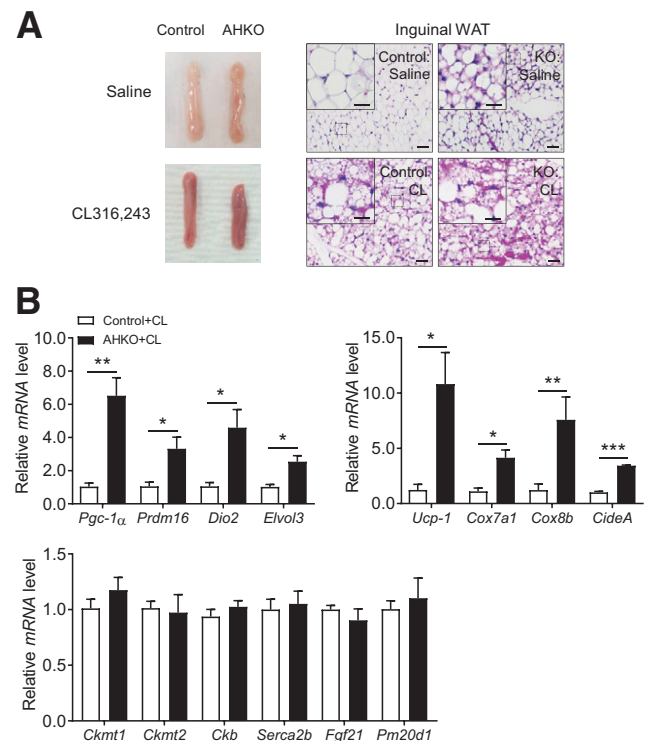
Figure 2—Mice lacking AHKO exhibit increased energy expenditure. Mean average heat production (A), VO_2 consumption rates (B), RER (C), and activity level (D) determined at 14 weeks of age by indirect calorimetry in metabolic chambers during the 3-day measurement (after an initial 48 h of acclimation period). Dark- and light-phase cumulative means within dark or light phase and each time point were compared by Student t test between AHKO mice and their littermate male control mice. Data are presented as mean ± SEM. *$P < 0.05$. $n = 14$. BW, body weight; hr, hour.

on known pathways that lead to browning. We reasoned that beige cells induced by the loss in HOXC10 may be a key downstream event of β3-adrenergic receptor (AR)-cAMP signaling to promote adaptive thermogenesis in subcutaneous WAT depot. To test this, 10-week-old control and AHKO mice on chow diet were treated with the selective $β_3$-AR agonist CL-316,243 ([CL]) or saline for 7 days. Additional $β_3$-AR stimulation with CL (Fig. 3A) promoted browning of subcutaneous WAT in both control and AHKO mice compared with the groups treated with saline. Administration of CL to AHKO mice resulted in significantly increased expression of thermogenic markers and mitochondrial genes, but not Ucp-1–independent thermogenic genes, in subcutaneous WAT compared with control mice treated with CL (Fig. 3B); this increase in thermogenic gene expression profile was more pronounced compared with control and AHKO mice before CL treatment (Fig. 1F). We also examined all major adipose depots of AHKO mice maintained on chow diet. In these animals, morphological and molecular thermogenic genes in gonadal WAT and BAT (Supplementary Fig. 4A–D) of AHKO mice were not different from those observed in control

were observed in Myf5 HKO mice (Supplementary Fig. 3A), with the exception of a modest reduction in lean mass (Supplementary Fig. 3B). Consistent with gene expression analysis, histology analysis revealed no obvious changes in adipocyte morphology in BAT or subcutaneous WAT (Supplementary Fig. 3C–H). Metabolic status was also observed to be similar between both genotypes (Supplementary Fig. 3I–N). These findings supported our previous findings (22) that HOXC10 has no effect on BAT function. Rather, our data suggest that deletion of HOXC10 regulates adaptive thermogenesis and energy expenditure specifically in subcutaneous WAT in vivo; however, an additional stimulus may be needed to fully activate the thermogenic properties of subcutaneous WAT in AHKO mice.

Loss of HOXC10 Leads to Activated Thermogenic Profile via Adrenergic Signaling

Thermogenic adipocytes rely on β-adrenergic signaling for their activation in vivo. To elucidate a potential mechanism for increased browning of subcutaneous WAT depot in AHKO mice, we probed for the effect of HOXC10 deficiency

Figure 3—β-AR activation leads to enhanced thermogenic function in subcutaneous WAT of AHKO mice. A: Representative H-E staining of inguinal WAT from control and AHKO mice before (top panels) or after (bottom panels) injection with CL to induce beiging. Scale bars = 20 μm. Insets illustrate a magnified view of the figures (scale bars = 100 μm). $n = 4$. B: Relative mRNA levels of brown-fat selective markers, mitochondrial genes, and Ucp-1–independent thermogenic markers in inguinal WAT of control and AHKO mice treated with CL. Data are presented as mean ± SEM. Student t test: *$P < 0.05$, **$P < 0.01$, ***$P < 0.001$. $n = 4$.

animals. Thus, activation of the thermogenic gene program in WAT of the AHKO mice was limited to the subcutaneous WAT depot. We noticed that CL treatment resulted in reduced expression of several brown markers in BAT (Supplementary Fig. 4E and F) of AHKO mice compared with the control mice, which could be attributed to the presence of elevated basal level of β_3-adrenergic activation in subcutaneous WAT of AHKO mice. Taken together, these results suggest that the effects of HOXC10 deficiency on browning of subcutaneous WAT are, at least in part, mediated via activated β_3-adrenergic signaling.
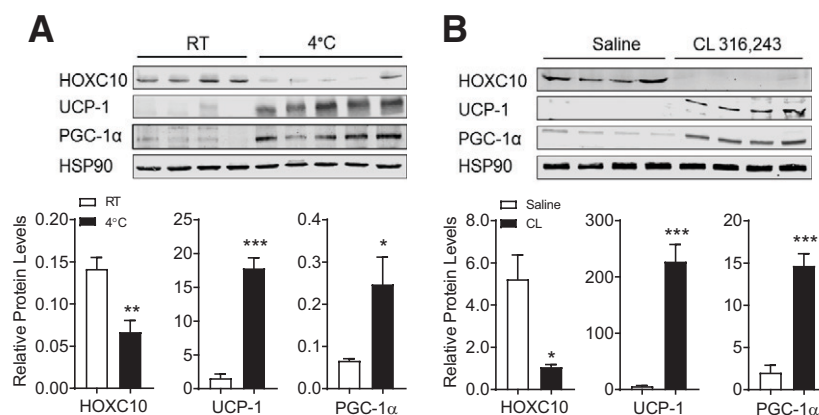
Translational Regulation of *HOXC10* in Subcutaneous WAT by Cold Exposure and β_3-Adrenergic Signaling

The robust accumulation of beige adipocytes in AHKO mice suggest that HOXC10 suppresses thermogenic function in WAT, and its loss promotes remodeling of WAT and browning. To examine whether suppression of HOXC10 is a mechanistic event controlling thermogenic activation, we measured HOXC10 expression levels in subcutaneous WAT depot of C57BL6/J mice housed at room temperature or 4°C for 7 days. Prolonged cold challenge for 7 days did not decrease *HOXC10* mRNA level, while HOXC10 protein levels were strongly decreased (Fig. 4A and Supplementary Fig. 5A). The loss of HOXC10 protein in subcutaneous WAT corresponded to an increase in PGC-1α and Ucp-1 protein levels. Similar results were observed in mice treated with CL for 7 days (Fig. 4B). The reduction of HOXC10 protein levels, but not mRNA levels, upon cold exposure or CL treatment (Supplementary Fig. 5) suggests a functional link between HOXC10 and proteasomal activity in subcutaneous WAT depots.

To investigate whether cold adaptation was linked to proteasome function, we measured proteasomal activity in both subcutaneous WAT and BAT from WT C57BL6/J

mice adapted to room temperature (22°C) or cold (4°C) for 7 days. Cold adaptation was associated with higher proteasomal activity in both depots, with greater proteasomal activity in subcutaneous WAT versus BAT (Fig. 5A), when compared with that after adaptation to room temperature. This observation demonstrated that proteasome function is critical for sustaining nonshivering thermogenesis in subcutaneous WAT. To pinpoint whether the ubiquitin-proteasome pathway is involved in regulating HOXC10 stability, we performed an in vivo ubiquitination assay and observed a typical smear of polyubiquitin conjugates in the presence of MG132 when probed with antiubiquitin antibody against the isolated Flag-tagged HOXC10 (pulldown by immunoprecipitation) (Fig. 5B). These data suggested that HOXC10 is polyubiquitinated in vivo.

E3 ligases perform the final step in ubiquitination and are critical for determining the specific recognition of the target protein for covalent attachment of ubiquitin. We performed a stable isotope labeling by/with amino acids in cell culture experiment to identify the possible E3 ligases for HOXC10 and found that E3 ligases KCTD2, KCTD5, and KCTD17 were potential interacting partners with HOXC10 when compared with control mouse IgG (Supplementary Table 1, L3). We next verified if HOXC10 could bind to these E3 ligases. Western blots of immunoprecipitation samples of Flag-tagged HOXC10 showed that KCTD2, KCTD5, and KCTD17 was capable of interacting with HOXC10 under forskolin-stimulation conditions compared with untransfected controls (Fig. 5C, black and blue arrowheads, respectively; band intensity of KCTD2 was relatively less in comparison with KCTD5 and KCTD17). We then repeated the ubiquitination assay and confirmed that cotransfection of HOXC10, ubiquitin, and KCTD2, 5, and 17 and immunoprecipitation of HOXC10 resulted in a smear of polyubiquitin conjugates

Figure 4—HOXC10 protein is translationally regulated in subcutaneous WAT by cold exposure and β_3-adrenergic activation. Immunoblot and densitometry analysis of endogenous HOXC10 protein in inguinal WAT isolated from WT C57BL6/J mice held at room temperature (RT) or exposed to 4°C (A) or treated daily with CL (1 mg/kg) or vehicle (saline) for 7 days (B) (n = 4–5 mice/group). HSP90 served as a loading control. Data are presented as mean ± SEM. Student t test: *P < 0.05, **P < 0.01, ***P < 0.001.

Figure 5—Physiological regulation of white adipocyte HOXC10 through cAMP-dependent PKA activation. *A*: Proteasome activity per inguinal WAT from WT mice after adaptation to room temperature (RT) or cold (4°C) for 7 days (*n* = 6 mice/group). *B*: In vivo ubiquitination assay on HeLa cells transfected with hemagglutinin (HA)–tagged ubiquitin and Flag-tagged HOXC10 expression vectors for 24 h, treated with forskolin (10 μm), followed by immunoprecipitations (IP) using FLAG antibody (M2) beads. Immunoblots (IB) were done on IP-lysate samples using anti-ubiquitin (to monitor ubiquitin conjugates on HOX10) and anti–Flag-HRP (to monitor successful transfection) antibodies. Flag-tagged p53 (Flag-p53) cotransfected with HA-ubiquitin was a positive (+ve) loading control for polyubiquitination. *n* = 4

(Fig. 5*D*, IP: Flag panel, rightmost lane). As KCTD2/5/17 antibody is raised against KCTD5 but also cross-reacts with KCTD2 and KCTD17, KCTD5 is primarily shown in the KCTD2/5/17 blot.

To ascertain that cold-induced decrease in HOXC10 abundance was due to increased protein degradation, we performed a cycloheximide chase assay in mature 3T3-L1 adipocytes overexpressing human HOXC10. Treatment of forskolin (mimicking cAMP-mediated cold-induced thermogenic response) accelerated the degradation of HOXC10, as evidenced by the reduced half-life when compared with control group (Fig. 5*E*). On the contrary, inhibiting cAMP-dependent protein kinase (PKA) activity with H89 prevented HOXC10 degradation in the presence of forskolin. Assessment of *Ucp-1* mRNA level at similar time points confirmed that, in the presence of forskolin where HOXC10 was degraded, *Ucp-1* expression was induced. Similarly, the reversal of HOXC10 protein degradation in the presence of H89 corresponded to a reduction in *Ucp-1* mRNA levels. These data demonstrated that cold-induced proteasome-mediated degradation of HOXC10 occurs in a PKA-dependent manner, which likely accounts for cold-induced increase in thermogenic *Ucp1* expression.

DISCUSSION

White and brown adipocytes share common mechanisms of induction in the process of browning. Several BAT-enriched transcription factors, including Prdm16, PGC-1α, Cebp-β, and Ebf2, have been identified to promote thermogenic program in classical BAT and WAT. However, there is a lack of identification of specific regulators of brown remodeling in subcutaneous fat depot. Our current study reveals that HOXC10 is a crucial negative regulator of white to beige fat transition in white adipocytes. We present biochemical and physiological data demonstrating that HOXC10 is critical for adipocyte biology and metabolism. We show that genetic deletion of HOXC10 in mice is associated with upregulation of the expression of *Ucp-1* and other genes critical for beige cell biogenesis in subcutaneous WAT, with no change in body weight, length, or composition. Furthermore, we show that HOXC10

depletion is associated with expansion of beige cells with a multilocular phenotype in subcutaneous WAT without effect on other fat depots and overall increased energy expenditure and improved glucose homeostasis, which overall impart an advantageous metabolic profile. The increased presence of beige adipocytes and increased energy expenditure correlate with the improved cold tolerance and glucose metabolism observed in these AHKO mice. We also reveal a mechanism that acts at the level of mature white adipocytes to suppress the thermogenic function of beige adipocytes. Our data together reveal a previously unknown function of HOXC10 in fat metabolism and suggest that promoting HOXC10 protein degradation may represent a potential therapeutic pathway in treating metabolic diseases.

Many genes and pathways that drive brown-fat thermogenesis have been demonstrated in previously established genetic mouse models of lean phenotypes and resistant to diet-induced obesity. For instance, ablation of cold-inducible regulators Prdm16, PPAR-α, PGC1-α, Zfp516, IRF4, EHMT1, and H2.0-like homeobox (Hlx) shows abnormal inhibition of BAT activity (23,30–35). Several of these positive regulators of classical BAT are also involved in regulating browning of murine WAT. On the contrary, the transcriptional regulator Zfp423 was reported to inhibit the activity of Ebf2 and suppress Prdm16 activation in white adipocytes, thus suppressing thermogenic gene program in WAT (36). A recent study further demonstrated that the cyclin-dependent kinase 6 (CDK6) inhibits white to beige fat transition by suppressing Runt-related transcription factors (RUNX1) that normally promote *Ucp-1* and *Pgc-1α* expression (37). We previously identified HOXC10 as a suppressor of brown fat gene expression in subcutaneous WAT (22). This was demonstrated using in vitro model of white adipocytes, including differentiated 3T3-L1 and SVF isolated from white adipocytes. Our AHKO transgenic mouse model presented enhanced thermogenic capacity under room temperature conditions when fed on chow diet, with minimal effect on WAT genes. Thus, HOXC10 has no effect on adipogenesis per se. Instead, significant beige adipocyte formation was observed specifically in the subcutaneous WAT, not in other fat depots, as supported by in vitro knockdown primary cell culture studies and in vivo adipose

---

independent in vivo ubiquitination experiments. *C*: HEK293T cells transfected with Flag-tagged HOXC10, V5-tagged KCTD2, Myc-tagged KCTD5, and HA-tagged KCTD17 expression vectors for 48 h, treated with forskolin (10 μm), and followed by IP using FLAG antibody (M2) beads. Immunoblots were performed on input and IP samples using anti-Flag, anti-V5, anti-Myc, anti-HA, and anti-KCTD5 antibodies. Anti-KCTD5 antibody preferentially detected KCTD5 (26 kDa, black arrowheads), but was also able to detect KCTD2 and KCTD17 (29 kDa and 37 kDa, black and blue arrowheads, respectively). HSP90 was used as a loading control; *n* = 3 independent replicates. *D*: Repeat of *B* above, using HeLa cells transfected with HA-tagged ubiquitin (Ubq), Flag-tagged HOXC10, and KCTD2, 5, and 17 expression vectors for 24 h, followed by IP using FLAG antibody (M2) beads. Immunoblots were done on IP-lysate samples using anti-ubiquitin (to monitor ubiquitin conjugates on HOXC10), anti-Flag, anti-KCTD (to monitor successful transfection), and anti-HSP90 (loading control) antibodies; black arrowheads show the preferentially detected KCTD5 protein band. *n* = 3 independent in vivo ubiquitination experiments. *E*, left: Differentiated 3T3-L1-FlagHOXC10 cells were treated with cycloheximide (CHX; 100 μg/ml), forskolin (10 μm), or H89 (50 μmol/L) for the indicated hours (hr). The remaining HOXC10 at different time points was quantified as the percentage of initial HOXC10 level (0 h of CHX treatment). *Statistically different between control and forskolin-treated; #statistically different between forskolin and H89-treated. HSP90 served as a loading control. *E*, right: Corresponding Ucp-1 mRNA expression following treatment with CHX and forskolin. *n* = 4 independent CHX chase assays. Data are presented as mean ± SEM. Student *t* test: *$P < 0.05$, **$P < 0.01$, ***$P < 0.001$. AU, arbitrary units.

depot–specific delivery of HOXC10 virus injection studies. Moreover, these mice exhibited increased energy expenditure and enhanced glucose tolerance. The enhanced ability to maintain body temperature to prolonged cold exposure suggests that heat production by beige adipocytes is facilitated by the upregulation in *Ucp-1* gene levels in subcutaneous WAT in AHKO mice, indicating that remodeling of subcutaneous WAT can be achieved in response to the loss of HOXC10. In this regard, it is important to note that a recent study demonstrated that Zfp423, a negative regulator of browning in white adipocytes, protects mice against HFD-induced hepatic steatosis (36). Inactivation of Zfp423 promotes browning not only in subcutaneous WAT but also in gonadal WAT and partially reduced BAT function (36). This effect is attributed to Zfp423 inhibiting the actions of brown-fat determination factor Ebf2, thus suppressing Prdm16 transcriptional activation. Given that Zfp423 favors the expression of BAT gene expression in both subcutaneous and gonadal WAT fat depots, the actions of Zfp423 potentially highlights the presence of distinct regulatory machineries that govern overall WAT function, while HOXC10 is mainly involved in the process of browning in subcutaneous WAT. In addition, we noted that deletion of HOXC10 specifically in BAT in Myf5 KO mice had no significant effect on brown-fat gene expression and did not affect BAT function. This finding is in agreement with our previous study, confirming that HOXC10 acts mainly to suppress brown fat genes and primarily regulates the process of browning in mature subcutaneous WAT without affecting other fat depots. Taken together, our findings establish HOXC10 as a selective white adipocyte marker, which plays a major role in governing the process of browning of subcutaneous WAT.

Cold exposure and β_3-AR agonists promote the expression of brown-fat thermogenic genes through the cAMP-dependent PKA activation signaling cascade (38). Thus, we focused on mechanisms by which the beige adipocyte thermogenic program is regulated by HOXC10 following cold-induced cAMP activation. Consistent with our previous study (22), HOXC10 protein expression is suppressed in subcutaneous WAT upon prolonged cold exposure. A consistent downregulation in HOXC10 expression in vivo is also observed in the same fat depot upon pharmacological activation of β_3-AR, suggesting that the loss of HOXC10 protein may represent an intrinsic mechanism by which thermogenic adipocytes becomes activated following cold exposure or activation of β_3-AR. In both models of browning, we observed reduced HOXC10 protein level, but not the mRNA level. The protein abundance of HOXC10 is inversely correlated with thermogenic genes in subcutaneous WAT, suggesting that the turnover of HOXC10 beyond its transcriptional regulation, is targeted for proteolysis through the ubiquitin-proteasome pathway. In this context, we found that cold adaptation resulted in enhanced proteasomal activity in subcutaneous WAT and is likely responsible for promoting browning of subcutaneous WAT during cold acclimation. Mechanistically, cold exposure or forskolin treatment leads to the activation of PKA and resulted in proteasome-mediated degradation of HOXC10, likely mediated through the E3 ligases KCTD2, 5, and 17. Of note, this process was reversible, given that the PKA inhibitor H89 reversed HOXC10 protein degradation, indicating that HOXC10 degradation occurs downstream of PKA activation. We also observed a corresponding reduction in *Ucp-1* expression levels, thus emphasizing the adaptive role and mechanistic link between HOXC10, nonshivering thermogenesis, and proteasomal function. It is known that PKA activation causes protein phosphorylation, resulting in protein posttranslational modification. While we identified HOXC10 as a potential PKA substrate, complementary studies demonstrating the novel potential PKA phosphorylation sites of HOXC10 await further investigation. In addition, complementary experiments of AHKO mice under HFD feeding or thermoneutral conditions could provide more insights into the effects of the lack of HOXC10 on energy homeostasis in mice.

Adipocytes possess remarkable adaptive plasticity in response to environmental cues to sustain proper systemic metabolic health. Given difficulties to promote or sustain weight loss in obese patients, determination of physiological adaptations to promote adipocyte health will offer new avenues for the treatment of obesity-associated pathologies. Moreover, enhancing adaptive thermogenesis would increase energy expenditure and thus promote weight loss. Previously, our group has shown that regulation of HOXC10 is both sufficient and necessary for promoting browning of subcutaneous WAT (22). Expression of HOXC10 was shown to suppress genes associated with BAT and to suppress browning of WAT in vivo. HOXC10 was also shown to be able to interact with the 5' regulatory region of Prdm16 and mediates its effect partially through Prdm16 to regulate its function in the browning of subcutaneous WAT. In this study, we demonstrated that proteasome-mediated HOXC10 protein degradation, at least partially through the E3 ligases KCTD2, 5, and 17, is critical to the metabolic function of white adipocytes essential to secure systemic metabolic integrity. Future work will aim to further dissect HOXC10-associated transcriptional machinery and investigate in detail how metabolic and pathological conditions can impact HOXC10 translation and/or activity. In summary, we have found that cold induction or adrenergic signaling activates PKA and suppresses HOXC10 expression by increased proteasome-mediated degradation, likely through the E3 ligases KCTD2, 5, and 17. This loss of HOXC10 expression reverses the suppression of Prdm16 expression and therefore drives white adipocyte thermogenic function and promotes robust browning of subcutaneous WAT and thus may be a target in improving metabolic health in obesity and beyond.

Duality of Interest. No potential conflicts of interest relevant to this article were reported.

Author Contributions. H.Y.A.T. and M.F.M.S. performed experiments, analyzed data, and wrote the manuscript. S.-X.T., Y.N., S.Y.G., H.L., and S.P.N. performed experiments and analyzed data. J.G., F.X., and W.H. contributed to discussion and reviewed and edited the manuscript. All authors reviewed and edited the manuscript. W.H. is the guarantor of this work and, as such, had full access to all the data in the study and takes responsibility for the integrity of the data and the accuracy of the data analysis.

Prior Presentation. Parts of this study were presented in abstract form at the 79th Scientific Sessions of the American Diabetes Association, San Francisco, CA, 7–11 June 2019.

References

1. Cannon B, Nedergaard J. Brown adipose tissue: function and physiological significance. Physiol Rev 2004;84:277–359

2. Cypess AM, Lehman S, Williams G, et al. Identification and importance of brown adipose tissue in adult humans. N Engl J Med 2009;360:1509–1517

3. Nedergaard J, Bengtsson T, Cannon B. Unexpected evidence for active brown adipose tissue in adult humans. Am J Physiol Endocrinol Metab 2007;293:E444–E452

4. Virtanen KA, Lidell ME, Orava J, et al. Functional brown adipose tissue in healthy adults. N Engl J Med 2009;360:1518–1525

5. Wu J, Boström P, Sparks LM, et al. Beige adipocytes are a distinct type of thermogenic fat cell in mouse and human. Cell 2012;150:366–376

6. Cohen P, Levy JD, Zhang Y, et al. Ablation of PRDM16 and beige adipose causes metabolic dysfunction and a subcutaneous to visceral fat switch. Cell 2014;156:304–316

7. Wu J, Cohen P, Spiegelman BM. Adaptive thermogenesis in adipocytes: is beige the new brown? Genes Dev 2013;27:234–250

8. Harms M, Seale P. Brown and beige fat: development, function and therapeutic potential. Nat Med 2013;19:1252–1263

9. Shinoda K, Luijten IHN, Hasegawa Y, et al. Genetic and functional characterization of clonally derived adult human brown adipocytes. Nat Med 2015;21:389–394

10. Cypess AM, Weiner LS, Roberts-Toler C, et al. Activation of human brown adipose tissue by a β3-adrenergic receptor agonist. Cell Metab 2015;21:33–38

11. Lee P, Smith S, Linderman J, et al. Temperature-acclimated brown adipose tissue modulates insulin sensitivity in humans. Diabetes 2014;63:3686–3698

12. Ouellet V, Routhier-Labadie A, Bellemare W, et al. Outdoor temperature, age, sex, body mass index, and diabetic status determine the prevalence, mass, and glucose-uptake activity of 18F-FDG-detected BAT in humans. J Clin Endocrinol Metab 2011;96:192–199

13. Vijgen GHEJ, Bouvy ND, Teule GJJ, et al. Increase in brown adipose tissue activity after weight loss in morbidly obese subjects. J Clin Endocrinol Metab 2012;97:E1229–E1233

14. Trainor PA, Krumlauf R. Hox genes, neural crest cells and branchial arch patterning. Curr Opin Cell Biol 2001;13:698–705

15. Argiropoulos B, Humphries RK. Hox genes in hematopoiesis and leukemogenesis. Oncogene 2007;26:6766–6776

16. Naguibneva I, Ameyar-Zazoua M, Polesskaya A, et al. The microRNA miR-181 targets the homeobox protein Hox-A11 during mammalian myoblast differentiation. Nat Cell Biol 2006;8:278–284

17. Yutzey KE, Rhee JT, Bader D. Expression of the atrial-specific myosin heavy chain AMHC1 and the establishment of anteroposterior polarity in the developing chicken heart. Development 1994;120:871–883

18. Yutzey K, Gannon M, Bader D. Diversification of cardiomyogenic cell lineages in vitro. Dev Biol 1995;170:531–541

19. Mori M, Nakagami H, Rodriguez-Araujo G, Nimura K, Kaneda Y. Essential role for miR-196a in brown adipogenesis of white fat progenitor cells. PLoS Biol 2012;10:e1001314

20. Yoneyama S, Guo Y, Lanktree MB, et al.; Look AHEAD Research Group; GIANT Consortium; CARe IBC Consortium. Gene-centric meta-analyses for central adiposity traits in up to 57 412 individuals of European descent confirm known loci and reveal several novel associations. Hum Mol Genet 2014;23:2498–2510

21. Brune JE, Kern M, Kunath A, et al. Fat depot-specific expression of HOXC9 and HOXC10 may contribute to adverse fat distribution and related metabolic traits. Obesity (Silver Spring) 2016;24:51–59

22. Ng Y, Tan S-X, Chia SY, et al. HOXC10 suppresses browning of white adipose tissues. Exp Mol Med 2017;49:e292

23. Seale P, Conroe HM, Estall J, et al. Prdm16 determines the thermogenic program of subcutaneous white adipose tissue in mice. J Clin Invest 2011;121:96–105

24. Ohno H, Shinoda K, Spiegelman BM, Kajimura S. PPARγ agonists induce a white-to-brown fat conversion through stabilization of PRDM16 protein. Cell Metab 2012;15:395–404

25. Tchkonia T, Lenburg M, Thomou T, et al. Identification of depot-specific human fat cell progenitors through distinct expression profiles and developmental gene patterns. Am J Physiol Endocrinol Metab 2007;292:E298–E307

26. Considine RV, Sinha MK, Heiman ML, et al. Serum immunoreactive-leptin concentrations in normal-weight and obese humans. N Engl J Med 1996;334:292–295

27. Havel PJ, Kasim-Karakas S, Mueller W, Johnson PR, Gingerich RL, Stern JS. Relationship of plasma leptin to plasma insulin and adiposity in normal weight and overweight women: effects of dietary fat content and sustained weight loss. J Clin Endocrinol Metab 1996;81:4406–4413

28. Filozof CM, Murúa C, Sanchez MP, et al. Low plasma leptin concentration and low rates of fat oxidation in weight-stable post-obese subjects. Obes Res 2000;8:205–210

29. Cousin B, Cinti S, Morroni M, Raimbault S, Ricquier D, Pénicaud L, Casteilla L. Occurrence of brown adipocytes in rat white adipose tissue: molecular and morphological characterization. J Cell Sci 1992;103:931–942

30. Ohno H, Shinoda K, Ohyama K, Sharp LZ, Kajimura S. EHMT1 controls brown adipose cell fate and thermogenesis through the PRDM16 complex. Nature 2013;504:163–167

31. Dempersmier J, Sambeat A, Gulyaeva O, et al. Cold-inducible Zfp516 activates UCP1 transcription to promote browning of white fat and development of brown fat. Mol Cell 2015;57:235–246

32. Hondares E, Rosell M, Díaz-Delfín J, et al. Peroxisome proliferator-activated receptor α (PPARα) induces PPARγ coactivator 1α (PGC-1α) gene expression and contributes to thermogenic activation of brown fat: involvement of PRDM16. J Biol Chem 2011;286:43112–43122

33. Kong X, Banks A, Liu T, et al. IRF4 is a key thermogenic transcriptional partner of PGC-1α. Cell 2014;158:69–83

34. Huang L, Pan D, Chen Q, et al. Transcription factor Hlx controls a systematic switch from white to brown fat through Prdm16-mediated co-activation. Nat Commun 2017;8:68

35. Puigserver P, Wu Z, Park CW, Graves R, Wright M, Spiegelman BM. A cold-inducible coactivator of nuclear receptors linked to adaptive thermogenesis. Cell 1998;92:829–839

36. Shao M, Ishibashi J, Kusminski CM, et al. Zfp423 maintains white adipocyte identity through suppression of the beige cell thermogenic gene program. Cell Metab 2016;23:1167–1184

37. Hou X, Zhang Y, Li W, et al. CDK6 inhibits white to beige fat transition by suppressing RUNX1. Nat Commun 2018;9:1023

38. Zhang G, Sun Q, Liu C. Influencing factors of thermogenic adipose tissue activity. Front Physiol 2016;7:29